Chapter 5

Clerodendron glandulosum.Coleb leaf extract prevents in vitro human LDL oxidation ,macrophage differentiation and oxidized LDL induced foam cell formation and apoptosis in macrophages

INTRODUCTION

Atherosclerosis, a cardiovascular disorder with its increasing rate of mortality poses great challenge to developing and developed countries (Magdalena *et al.*, 2009). Many cell types such as macrophages, endothelial cells and smooth muscle cells possess the ability to oxidize LDL. Oxidation of LDL is crucial in plaque formation (Steinberg, 1997) as it induces differentiation of monocytes into macrophages, promotes LDL uptake by macrophages through their scavenger receptors and subsequently induces sub-endothelial lipid accumulation and foam cell formation, the earliest hallmarks of atherosclerosis (Steinberg *et al.*, 1989). Oxidized LDL serves as a chemo-attractant for circulating monocytes both directly as well as via stimulated release of monocyte chemo-attractant protein-1(MCP) from endothelial cells (Cushing *et al.*, 1990). It also serves as an attractant to T cells and motility inhibitor of resident macrophages (Young and McEneny, 2001). Unlike native LDL, oxLDL is immunogenic (Palinski *et al.*, 1989) and cytotoxic to various cell types, including endothelial cells. Asmis and Begley (2003) have reported cytotoxicity of oxLDL to monocyte derived macrophages consequent to its induced uptake by monocytes. Apparently, macrophage apoptosis plays a key role in the development of atherosclerotic lesion as, several studies have demonstrated macrophage apoptosis in human atheroma (Isner *et al.*, 1995; Kolodgie *et al.*, 1999). Available drugs such as statin (hypocholesterolemic agent), aspirin (anti-platelet agent), beta-blockers, ACE (angiotensin-converting enzyme) inhibitors, calcium channel blockers etc. all cause apparent side effects. Even surgical interventions such as angioplasty, endarterectomy, thrombolytic therapy and bypass surgery are subject to post-operative trauma and often fail to achieve desired results. An anti-atherosclerotic role for both vitamin C and E has found mention in recent times of which, particularly vitamin E

appears capable of retarding LDL oxidation and inhibit proliferation of smooth muscle cells, platelet aggregation and expression of adhesion molecules.

In this context, natural remedies in the form of herbal interventions beg serious evaluation as effective, safe and less expensive alternatives for treatment of atherosclerosis. Due to their competence to prevent LDL oxidation (Chang *et al.*, 2006; Chu *et al.*, 2009) and plaque formation (Ho *et al.*, 2010), plant extracts, food supplements or spices with reported antioxidants and lipid lowering properties are promising prospects for combating atherosclerosis. Wild betel - *Piper sarmentosum* (Amran *et al.*, 2010), purple sweet potato – *Ipomoea batatas* (Park *et al.*, 2010), Andawali - *Tinospora crispa* (Zulkhairi *et al.*, 2010), Bilberry - *Vaccinium myrtillus* (Mauray *et al.*, 2010) are some potential anti-atherogenic candidates reported recently.

Aim: - The present study in this behest, investigates the efficacy of aqueous extract of CG leaves as an anti-atherosclerotic agent using *in vitro* experimental models.

MATERIALS AND METHODS

Plant, preparation of extract and phytochemical analysis

As mentioned in chapter 1

Isolation of human LDL

Venous blood collected from fasted individuals kept at room temperature for 45 minutes and centrifuged at 3000 rpm for 10 min at 4°C yielded serum. Heparin-citrate buffer (0.064 M tri sodium citrate at pH 5.05 containing 50,000 IU/l heparin) precipitation method of Ahotupa *et al.* (1998) helped isolate LDL. A mixture of 1 ml of heparin-citrate buffer and 0.1ml of serum was vortex mixed and allowed to stand for 10 min at room temperature. The insoluble lipoproteins sedimented as a pellet by

centrifugation at 3000 rpm for 10 min (at 20°C) was suspended in 1 ml PBS (0.1 M, pH 7.4, containing 0.9% NaCl). The method of Lowry *et al.* (1951) using bovine serum albumin as standard helped estimate the LDL protein content.

LDL oxidation kinetics

Hundred micro litre of LDL (100-µg protein) was diluted to 0.9 ml with PBS and incubated with or without 100 µl of CG extract (20-200 µg/ml) at 37°C for 30 min. Addition of 10 µl of freshly prepared 0.167 mM $CuSO_4$ at the end of incubation initiated oxidation. The oxidation kinetics were determined by monitoring the change in absorbance at 234 nm every 10 min at 37°C for 3 h at 234 nm for the production of CD in a UV/VIS Perkin Elmer spectrophotometer as described by Esterbauer *et al.* (1989).

Lag time (min) was determined from the intercept of lines drawn through the linear portions of the lag and propagation phases. The rate of oxidation (expressed as nmol/min) was determined from the slope of the propagation phase. Maximum concentration of CD formed ($CD_{max.}$ = expressed as nmol/mg protein) was calculated from the difference in absorbance at zero time and at diene peak. The concentration of CD in the samples was availed by the usage of a molar extinction coefficient of 2.95 $\times 10^4$ M^{-1} cm^{-1} (Esterbauer *et al.* 1989).

Measurement of MDA, LHP and PC content

Three sets of tubes were prepared for LDL oxidation and copper mediated LDL oxidation and assessed in presence or absence of CG extract (10-200 µg/ml) for 24 h as mentioned above. The tubes were then processed for measurement of MDA, LHP and PC after stopping oxidation by adding 10 µl of 10 mM EDTA.

For MDA measurement, 100 µl aliquot was mixed with 1 ml TBA reagent (0.37% TBA, 15% TCA in 0.25 N HCl) and placed in water bath at 100°C for 30 min,

cooled to room temperature and centrifuged at 3000 rpm for 10 min. The absorbance of the supernatant was measured at 532 nm with UV/VIS Perkin Elmer spectrophotometer and, MDA was calculated using a molar absorption coefficient of 1.56×10^5 M^{-1} cm^{-1} (Buege and Aust, 1978).

For LHP estimation, 100-µl aliquot mixed with 0.9 ml of Fox reagent (250-µM ammonium sulphate, 100-µM xylenol orange, 25 mM H_2SO_4 and 4 mM butylated hydroxyl toluene in 90% (v/v) HPLC-grade methanol) was incubated at 37 °C for 30 min. The developed colour read at 560 nm yielded LHP content by using the molar absorption coefficient of 4.3×10^4 M^{-1} cm^{-1} (Nourooz-Zadeh *et al.*, 1996).

For PC estimation, 0.1ml aliquot was mixed with 0.2ml of DNPH (in 2 M HCl). After incubation at room temperature for 1 h, 0.6ml denaturing buffer (0.15 M sodium phosphate buffer containing 3% SDS) was added and mixed thoroughly. Then ethanol and heptane (1.8 ml of each) were added, mixed for 1 min, and centrifuged to precipitate protein. The protein was washed three times with 1.5 ml ethyl acetate/ethanol (1/1, v/v) and dissolved in 1ml denaturing buffer and read at 360 nm in a spectrophotometer. The carbonyl content was calculated from the absorbance (360 nm) using an absorption coefficient ε of 22.000 $M^{-1}cm^{-1}$ (Reznick and Packer, 1994).

Relative Electrophoretic Mobility Assay

Copper mediated LDL oxidation was carried out in presence or absence of CG extract (10-200 µg/ml) for 24 h as mentioned above. The electrophoretic mobility of native or oxidized LDL (with or without CG extract) was detected, by agarose gel electrophoresis (Reid and Mitchinson, 1993). Samples were loaded on 0.6% agarose gel and electrophoresed (100 V) in 50mM barbituric acid (pH 8.6) for 30 min. After electrophoresis, the gels were fixed in a solution containing 60% methanol, 30%

water, and 10% glacial acetic acid for 30 min. The gels were then dried at 50°C for 40 min in a hot air oven and stained with 0.6% Sudan black B for 60 min and photographed. The result was expressed in terms of distance moved from origin.

ApoB Fragmentation Assay

Copper mediated LDL oxidation was carried out in presence or absence of CG extract (10-200 µg/ml) for 24 h as mentioned above. The LDL samples were denatured with 3% SDS, 10% glycerol, and 5% bromophenol at 95 °C for 10 min. Later, LDL samples were subjected to SDS-PAGE (8 %) electrophoresis at 100 V for 60 min and the gels were stained with Coomassie Brilliant Blue (Lee *et al.*, 2002).

Preparation of oxidized LDL and Human monocyte derived macrophage (HMDM)

Hundred micro litre of LDL (100µg protein) diluted to 900 µl with PBS was incubated for 24 h at 37°C subsequent to initiation of oxidation by 10 µl of freshly prepared 0.167 mM $CuSO_4$. Analysis of MDA and CD was the carried out in the LDL samples. Samples with MDA 50±5 nmol/mg LDL protein and CD 80±8 nmol/mg LDL protein were used for further studies.

THP-1, human monocyte cell line, was purchased from National Centre of Cell Sciences, Pune (INDIA). Cells were cultured in RPMI-1640 medium supplemented with 10% FBS and 1 % antibiotic-antimycotic solution in a humidified incubator with 5% CO_2. THP-1 monocyte cells were differentiated into macrophages by the addition of 50 nM phorbol 12-myristate 13-acetate (PMA) for 48 h (Park *et al.*, 2007). After differentiation to macrophages, the PMA-containing medium was replaced with serum-free medium and the cells were cultured for another 24 h before treatment.

Cell mediated LDL oxidation

HMDMs ($1x10^5$/24 mm well) underwent incubation in 1 ml of Ham's F-12 medium (without phenol red) containing nLDL (100µg/ml) with or without CG extract at 37°C for 24 hr. Cell free control well was used for all conditions. At the end of incubation, oxidation was arrested by chilling the medium and adding 200µM EDTA and 40µM BHT. Hundred µl of each supernatant was used for the assay of MDA and CD as described earlier (Duell *et al.*, 1998).

In vitro monocyte-macrophage differentiation

Human monocyte cell line (THP-1) were cultured in RPMI-1640 medium supplemented with 10% fetal bovine serum and 1 % antibiotic-antimycotic solution in a humidified incubator with 5% CO_2. THP-1 monocytes were differentiated into macrophages by the addition of 50 nM phorbol 12-myristate 13-acetate (PMA) for 48 h (Park *et al.*, 2007). The differentiation protocol was carried out on the cover slips placed in the 6 well culture plates. At the end of incubation period, cover slips from each well were collected, washed in PBS twice and immersed in 4% paraformaldehyde solution for 10 min followed by incubation in 3% hydrogen peroxide (to block endogenous peroxidase) for 20 min. At the end of incubation, non-specific sites were blocked by addition of 1% fetal bovine serum (20 min, at 4°C in humidified chamber), followed by incubation with mouse anti-human F4/80 primary antibody at 4°C in humidified chamber overnight. For visualization, cover slips were incubated with rabbit anti-mouse IgG-HRP; 1:100 (Bangalore Genei Pvt Ltd, INDIA) secondary antibody for 4 hr in a humidified chamber (at 4°C). At the end of incubation, sections were thoroughly washed with PBS and final detection step was carried out using DAB detection system (Bangalore Genei Pvt Ltd, INDIA) as the

chromagen and sections were counter-stained with haematoxylin. Sections were photographed using a canon Power shot S 70 digital camera under Leica DMRB microscope.

Ox-LDL induced foam cell formation

HMDMs pre-treated with CG extract (200µg/ml) for 30 min were incubated in presence of 100 µg/ml of Ox-LDL for 24 hr. Later, medium was decanted and cells fixed in 4 % paraformaldehyde for 15 min. The cells were then stained with 1% Oil red O solution for 30 min after washing twice with PBS. At the end of staining, excess Oil red O was removed and 1 ml of glycerine added. Photographs were taken on Leica DMIL inverted microscope using canon power shot S 70 digital camera.

Ox-LDL induced cytotoxicity of HMDMs

HMDMs pre-treated with CG extract (10-200µg/ml) for 30 min were incubated in presence of 100 µg/ml of Ox-LDL for 24 hr. Further incubation of the cells was carried out in a culture medium containing 0.5 mg/ml MTT for 4 h. Later, after addition of 150 µl of DMSO, all the wells were incubated for 30 min at room temperature with constant shaking. Absorbance was read at 540 nm using ELX800 Universal Microplate Reader (Bio-Tek instruments, Inc, Winooski, VT) and percentage of cell viability calculated subsequently.

Ox-LDL induced ROS generation in HMDMs

HMDMs pre-treated with CG extract (200µg/ml) for 30 min were incubated in presence of 100 µg/ml of Ox-LDL for 24 hr. Later, the cells further incubated for 1 h at 37°C and incubated with 7.5 µM DCF-DA for 30 min in dark (Silva *et al.*, 2010) were photographed using canon power shot S70 digital camera on Leica DMRB florescence microscope.

Measurement of mitochondrial membrane potential

The changes in mitochondrial membrane potential were measured using the fluorescent cationic dye Rhodamine 123 (rho123) as per Pereira and Oliveira, 2000. HMDMs pre-treated with CG extract (200µg/ml) for 30 min underwent incubation in presence of 100 µg/ml of Ox-LDL for 18 hr. The cells then underwent incubation with one µM rho123 for 10 min at 37°C. The fluorescence was determined at excitation and emission wavelengths of 485 and 530 nm, respectively using spectroflurometer (Jasco FP-6350).

Ox-LDL induced chromatin condensation in HMDMs

HMDM cells pre-treated with CG extract (200µg/ml) for 30 min, were incubated in presence of 100 µg/ml of Ox-LDL for 24 hr. Single-cell suspensions of treated HMDMs were washed with PBS, fixed in 70% ethanol for 20 min, and washed again with PBS. Cells were then incubated with DAPI stain (0.6µg/ml in PBS) for 5 min and washed with PBS for 5 min. Chromatin fluorescence was observed under a Leica DMRB 2000 florescence microscope. Apoptotic cells were morphologically defined by nuclear shrinkage and chromatin condensation (Hsieh *et al.*, 2007).

Ox-LDL induced alterations in cell cycle distribution in HMDMs

HMDMs pre-treated with CG extract (200µg/ml) for 30 min, were incubated in presence of 100 µg/ml of Ox-LDL for 24 hr. At the end of incubation, cells were collected, washed twice with PBS, fixed overnight in cold 70% ethanol at 4 °C and, re-suspended in PBS. Cells were incubated with RNase A for 45 min, and stained with propidium iodide (1 mg/ml) in the dark at 37 °C for 30 min (Pozarowski and Darzynkiewicz, 2004). The suspension was analysed on a flow Cytometer

(MoFlo™ Cytomation, Modular Flow Cytometer). The apoptosis was determined based on the "sub-G0" peak.

Annexin V-FITC/PI staining of Ox-LDL treated HMDMs

Annexin-V FITC/PI double-staining assay was used to quantify apoptosis, according to the manufacturer's protocol (Sigma Aldrich, Ltd.USA). HMDMs pre-treated with CG extract (200μg/ml) for 30 min, were incubated in presence of 100 μg/ml of Ox-LDL for 24 hr. The cells from each well were then centrifuged, washed with PBS and suspended in 100 μL binding buffer. Five μl of Annexin V FITC Conjugate and 10 μl of Propidium Iodide solution were added to each cell suspension and incubated for 10 min at room temperature in the dark. The samples were analysed on flow cytometer (MoFlo™ Cytomation, Modular Flow Cytometer) with CellQuest software. Double staining of cells with FITC-Annexin V and PI permits the discrimination of live cells ($FITC^-P^-$), early apoptotic ($FITC^+PI^-$), late apoptotic ($FITC^+PI^+$) or necrotic cells ($FITC^-PI^+$).

Statistical analysis

Statistical evaluation of the data was done by one-way ANOVA followed by Bonferroni's multiple comparison test. The results were expressed as mean ± S.E.M using Graph Pad Prism version 3.0 for Windows, Graph Pad Software, San Diego California USA.

RESULTS

LDL oxidation kinetics

As show in Figure 1, co-presence of CG extract significantly ($p<0.05$) increased the lag period for LDL oxidation and minimized CD_{max} formation and rate of LDL oxidation in a dose dependent manner compared to untreated LDL samples (Figure 1).

Measurement of TBARS, lipid hydroperoxides and protein carbonyl content

As shown in Figure 2, Cu^{2+} mediated LDL oxidation was characterized by elevated indices of TBARS, LHP and PC whereas, co-presence of CG extract significantly ($p<0.05$) minimized the production of TBARS, LHP and PC during LDL oxidation.

Relative Electrophoretic Mobility and ApoB fragmentation

Figure 3 shows the pattern of REM and ApoB fragmentation of Ox-LDL in presence or absence of CG extract. Co-presence of CG extract significantly prevented Cu^{2+} induced ApoB fragmentation. Cu^{2+} mediated LDL oxidation recorded 4.1 m REM compared to 1.3 of nLDL whereas, presence of CG extract recorded REM in the range of 3.8 to 1.3.

Cell mediated LDL oxidation

Incubation of nLDL with HMDMs for 24 hr resulted in significant increment in the indices of LDL-MDA and LDL-CD compared to control whereas, macrophage mediated LDL oxidation was significantly ($p<0.05$) prevented by the presence of CG extract as evidenced by the dose dependent decrement in the contents of LDL-MDA and LDL-CD (Figure 4).

Monocyte to macrophage differentiation

THP-1 human monocytes (suspension cells) were stimulated using PMA for 24 hr. Subsequent adhesion to the substratum and immunolocalization of macrophage cell surface marker (F4/80) was used as an index to determine the degree of macrophage differentiation. PMA-deprived monocytes did not differentiate and hence were not able to adhere on the substratum (Figure. 5). PMA treatment to THP-1 human monocytes resulted in higher number of F4/80 positive cells but, presence of CG extract recorded significant reduction of F4/80 positive cells indicating minimum differentiation of monocytes in to macrophages (Figure. 5).

In vitro foam cell formation

Incubation of HMDMs with Ox-LDL for 24 hr resulted in significant uptake of Ox-LDL, leading to higher intracellular cholesterol accumulation compared to control cells not exposed to Ox-LDL. Addition of CG extract to Ox-LDL treated macrophages significantly reduced Ox-LDL uptake by HMDMs (Figure 6).

Ox-LDL induced cytotoxicity and mitochondrial activity in HMDMs

Exposure of HMDMs to Ox-LDL resulted in significant decrement in cell viability ($p<0.05$) and increment in membrane depolarization ($p<0.05$) compared to untreated cells. However, Ox-LDL induced decrement in cell viability and increment in mitochondrial depolarization ($p<0.05$) were significantly minimized by the co-presence of CG extract in Ox-LDL exposed HMDMs (Figure 7)

Ox-LDL induced peroxyl radical generation and nuclear condensation

Exposure of HMDMs to Ox-LDL resulted in significant increment ($p<0.05$) in DCF-DA positive cells compared to control cells ($p<0.05$), however, co-presence of CG extract minimized Ox-LDL induced increment in peroxyl radical generation (minimal number of DCFDA positive cells). As shown in Figure 8, exposure of HMDMs to Ox-LDL showed greater number of cells (40% vs. 7% of control) with nuclear condensation while, co-presence of CG extract minimized the number of cells (13% vs. 40 % of Ox-LDL treated cells) with condensed nuclei (Figure 8).

Ox-LDL induced alteration in the cell cycle distribution and apoptosis in HMDMs

As shown in Figure 9, Ox-LDL exposed HMDMs recorded 24 % cells in the sub G0 phase (apoptotic) compared to 5.11 % cells in untreated HMDMs. However, Ox-LDL exposed HMDMs in presence of CG extract recorded only 12.00 % cells in sub G0 phase. In the annexine V-FITC/ PI staining assay, Ox-LDL treated HMDMs recorded 30.21% Annexine V positive (early apoptotic) and 12.18 % Annexine V and PI

positive cells (late apoptotic) compared to 5.45 % and 0.00 % in untreated and 16.55 % Annexine V positive and 6.76 % Annexine V and PI positive cells in presence of CG extract (Figure 10)

Figure.1 Effect of *C.glandulosum*.Coleb extract on kinetics of Cu^{2+} mediated LDL oxidation.

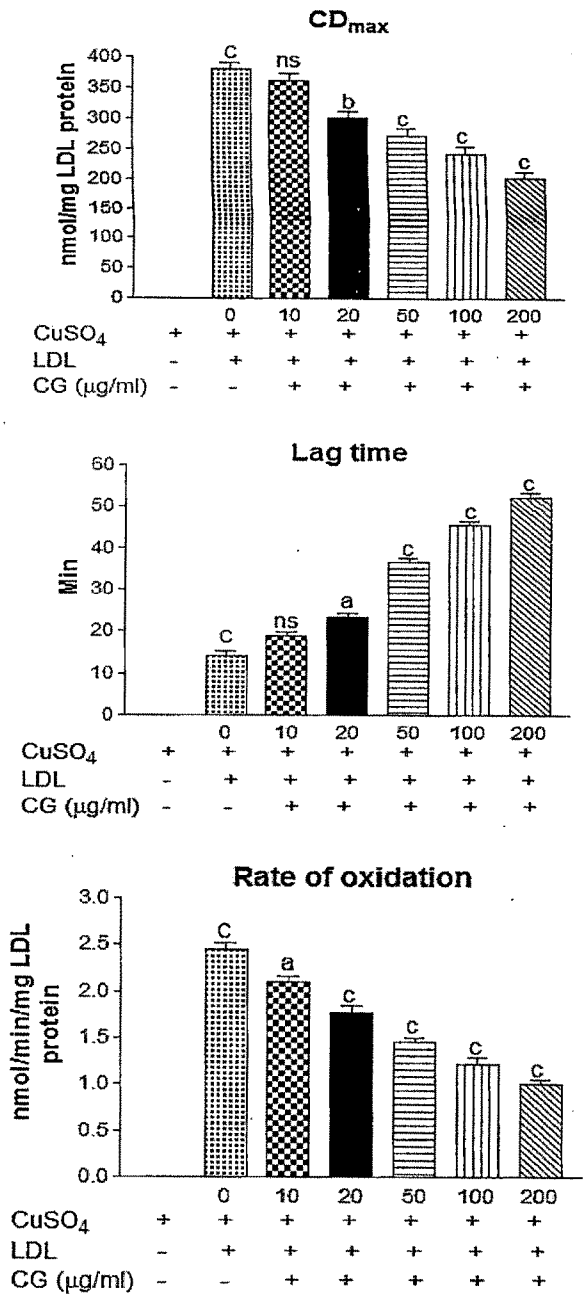

Data expressed as mean±S.E.M for n=3. $^{C}0<0.001$ compared to control ($CuSo_4$ alone) and $^{a}p<0.05$, $^{b}p<0.01$, $^{c}p<0.001$ and ^{ns}non significant compared to 0µg/ml CG.

Figure.2 Effect of *C.glandulosum*.Coleb extract on formation of oxidation products (MDA, LHP and PC) during Cu^{2+} mediated LDL oxidation.

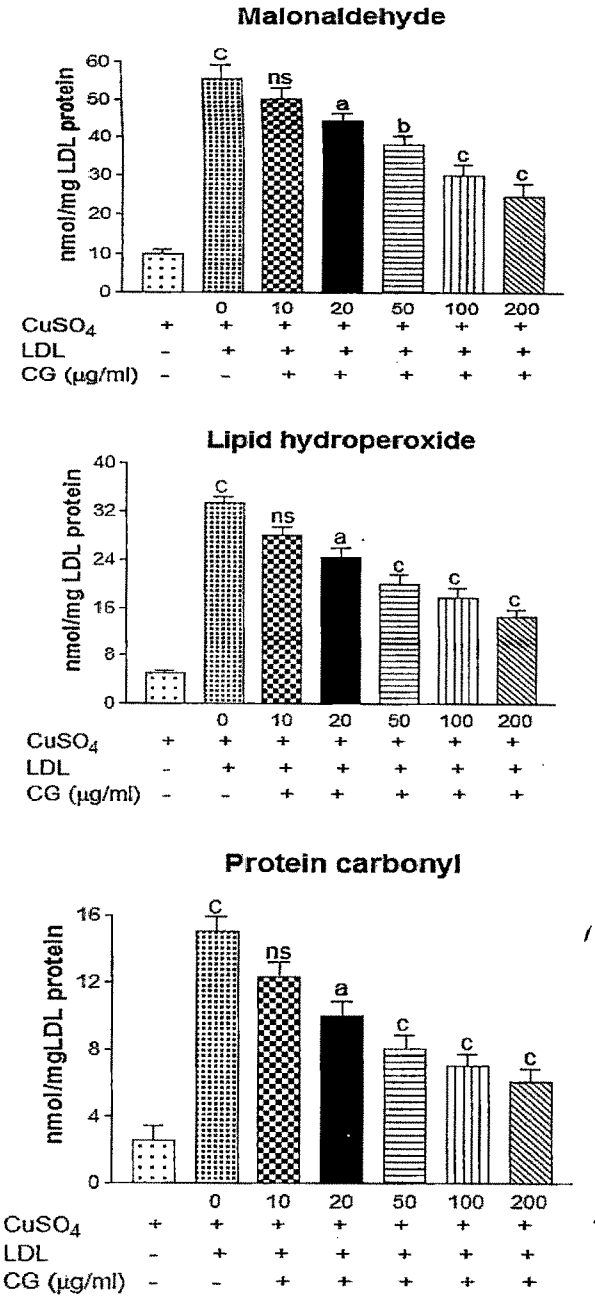

Data expressed as mean±S.E.M for n=3. $^{c}0<0.001$ compared to control ($CuSo_4$ alone) and $^{a}p<0.05$, $^{b}p<0.01$, $^{c}p<0.001$ and ^{ns}non significant compared to 0µg/ml CG.

Figure.3 Effect of *C.glandulosum*.Coleb extract on Cu^{2+} mediated alterations in relative electrophoretic mobility (REM) and ApoB fragmentation of LDL.

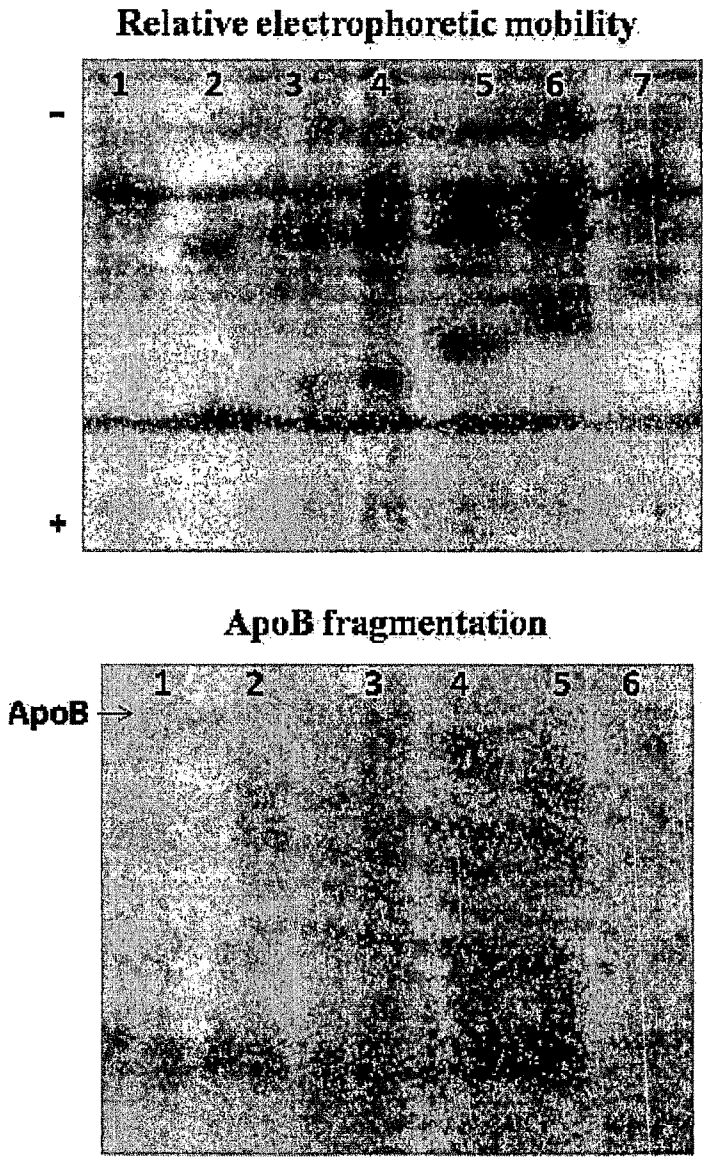

Where, 1: nLDL, 2: Ox-LDL, 3: Ox-LDL+10µg/ml CG, 4: Ox-LDL+20µg/ml CG, 5: Ox-LDL+50µg/ml CG, 6: Ox-LDL+100µg/ml CG and 7: Ox-LDL+200µg/ml CG.

Figure.4 Effect of *C.glandulosum*.Coleb extract on human monocyte derived macrophages (HMDMs) mediated LDL oxidation.

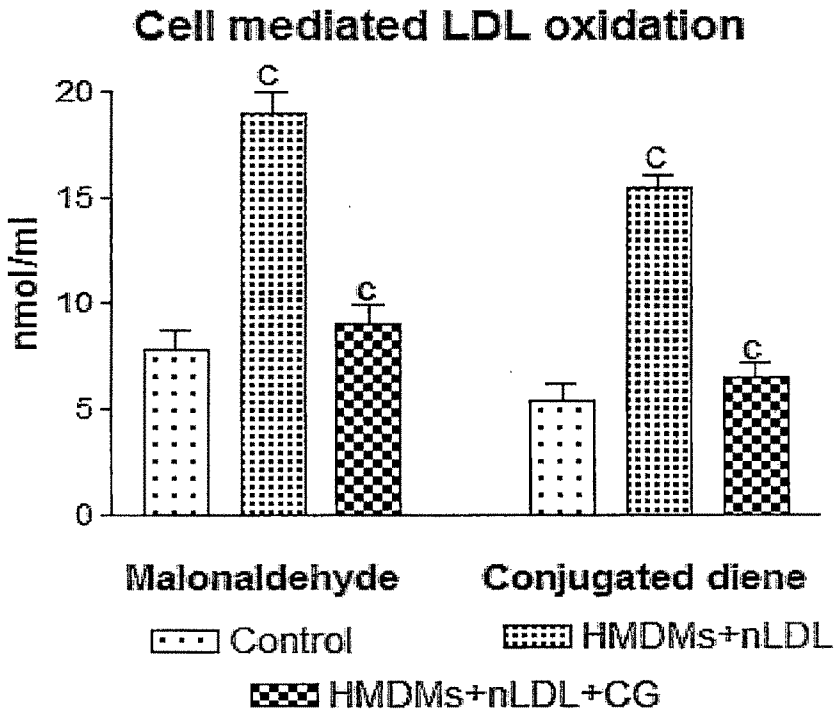

Control; Cell free supernatant, HMDMs+nLDL; supernatant collected from HMDMs exposed to nLDL and HMDMs+nLDL+CG; supernatant collected from HMDMs exposed to nLDL in presence of 200µg/ml CG extract
Data expressed as mean±S.E.M for n=3. $^{C}0<0.001$ compared to control ($CuSo_4$ alone) and $^{a}p<0.05$, $^{b}p<0.01$, $^{c}p<0.001$ and ^{ns}non significant compared to 0µg/ml CG.

Figure.5 Effect of *C.glandulosum*.Coleb extract on *in vitro* monocyte to macrophage differentiation (40X).

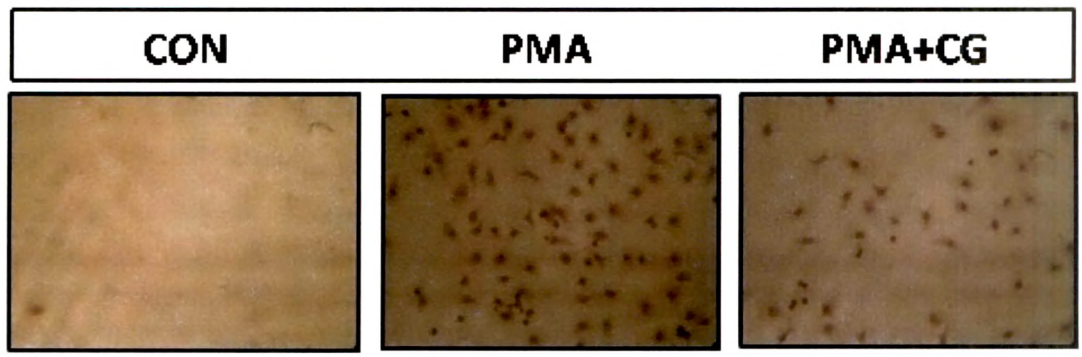

Where, CON; undifferentiated monocyte (THP-1 cells), PMA; THP-1 cells treated with phorbol-12-myristate-13-acetate, PMA+CG; THP-1 cells treated with phorbol-12-myristate-13-acetate in presence of 200µg/ml *C.glandulosum*.Coleb extract.

Figure.6 Effect of *C.glandulosum*.Coleb extract on Ox-LDL induced foam cell formation.

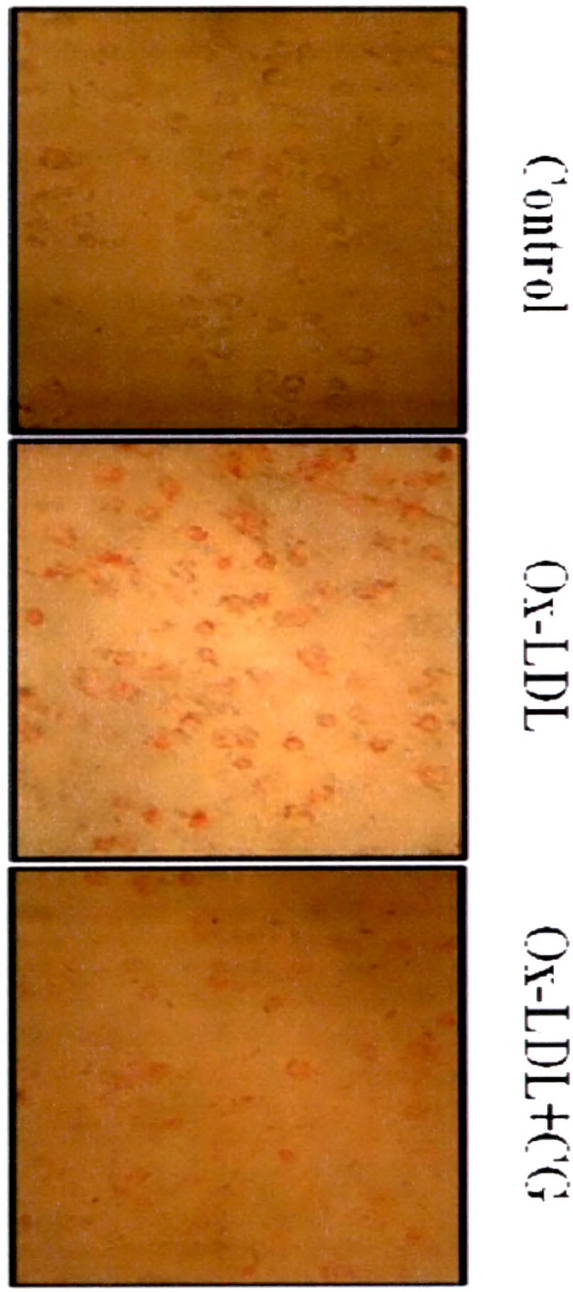

Control; HMDMs cells, Ox-LDL; HMDMs exposed to Ox-LDL and Ox-LDL+CG; HMDMs exposed to Ox-LDL in presence of 200µg/ml CG extract.

Figure.7 Effect of *C.glandulosum*.Coleb extract on cell viability and mitochondrial membrane potential in Ox-LDL exposed HMDMs.

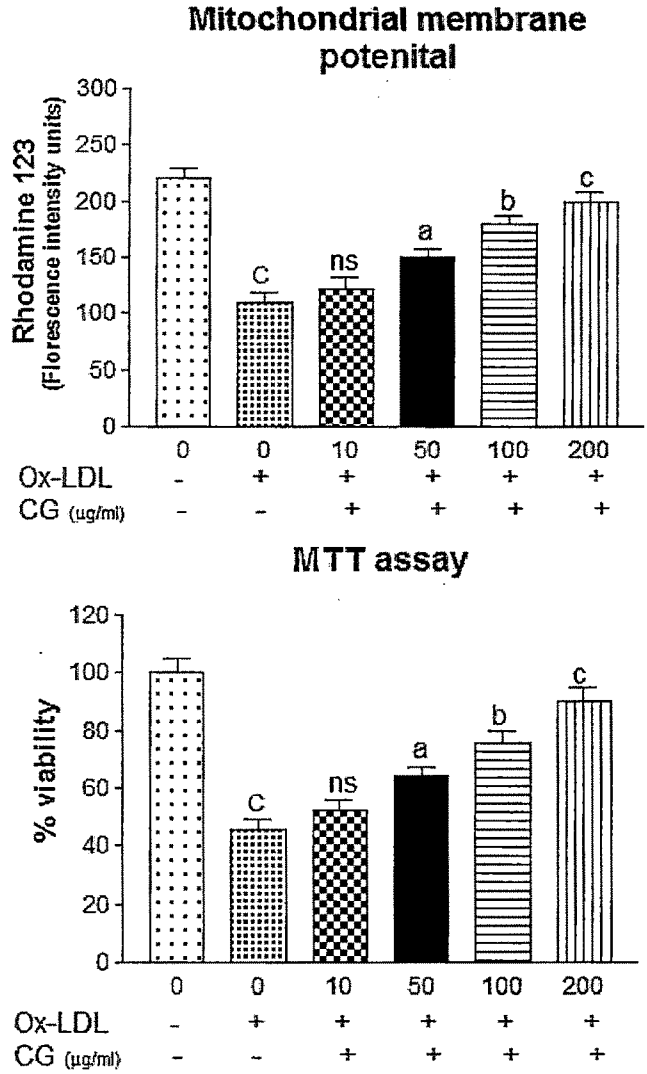

Data expressed as mean±S.E.M for n=3. $^{c}0<0.001$ compared to control ($CuSo_4$ alone) and $^{a}p<0.05$, bp<0.01, cp<0.001 and ^{ns}non significant compared to 0µg/ml CG.

Figure.8 Effect of *C.glandulosum*.Coleb extract on peroxyl radical generation (DCF-DA staining) and nuclear condensation (DAPI staining) in Ox-LDL exposed HMDMs.

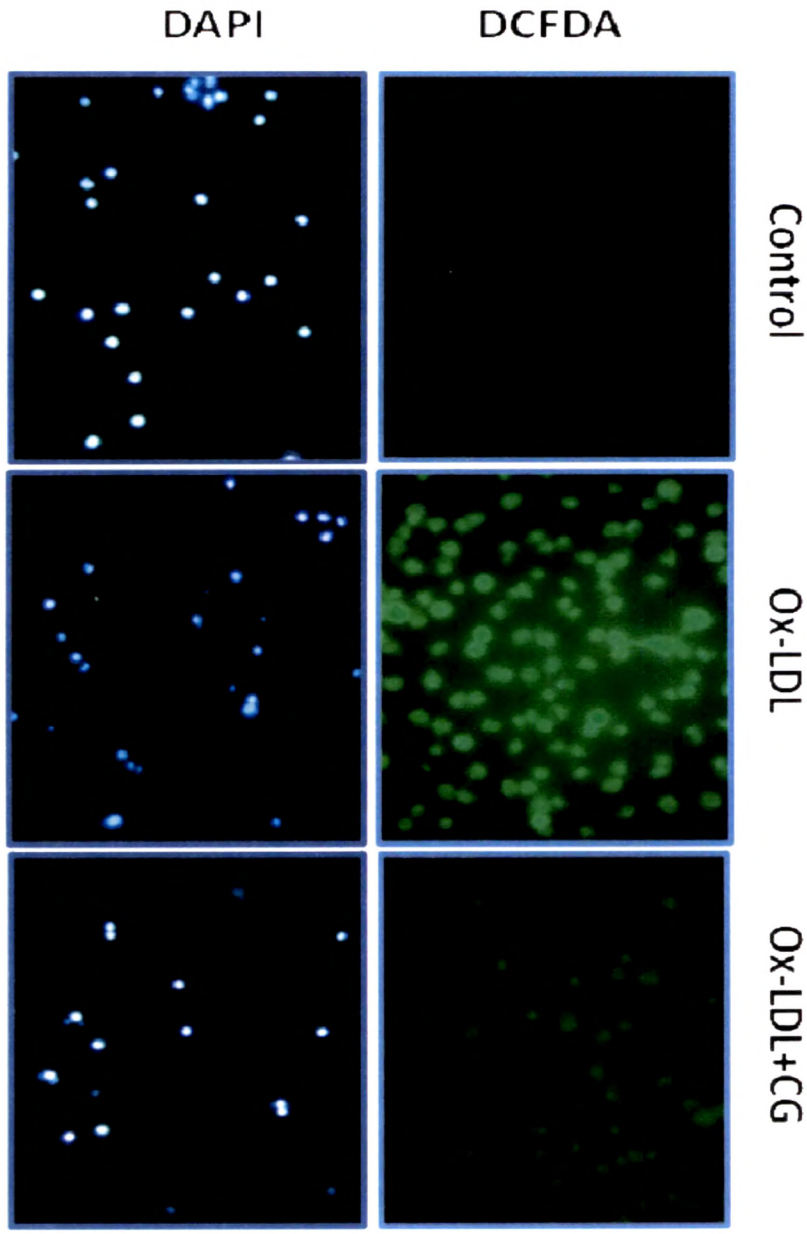

Control; HMDMs cells, Ox-LDL; HMDMs exposed to Ox-LDL and Ox-LDL+CG; HMDMs exposed to Ox-LDL in presence of 200µg/ml CG extract.

Figure.9 Effect of *C.glandulosum*.Coleb extract on cell cycle alterations in Ox-LDL exposed HMDMs.

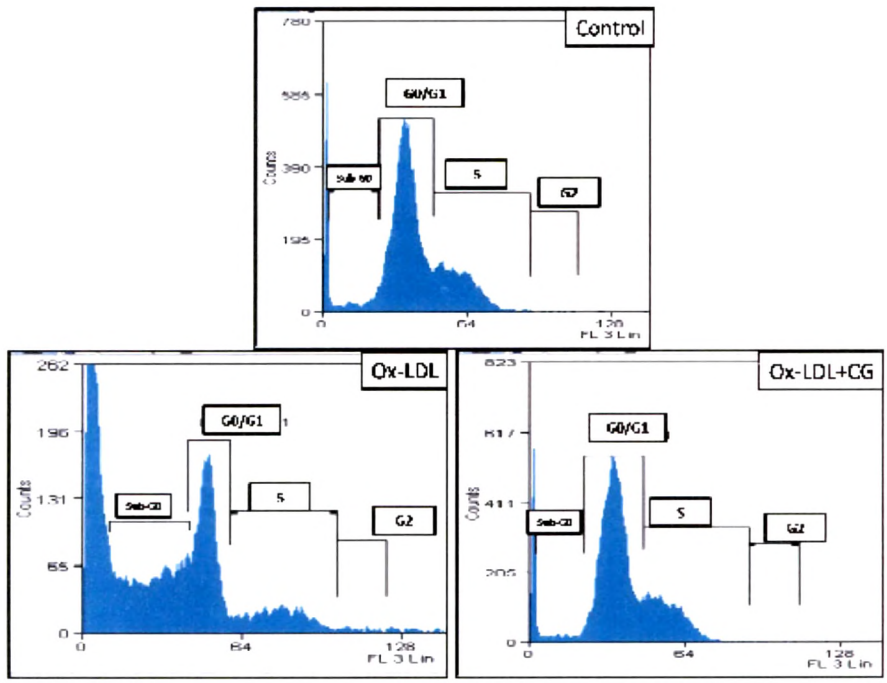

Control; HMDMs cells, Ox-LDL; HMDMs exposed to Ox-LDL and Ox-LDL+CG; HMDMs exposed to Ox-LDL in presence of 200µg/ml CG extract.

Figure.10 Effect of *C.glandulosum*.Coleb extract on apoptosis of Ox-LDL exposed HMDMs.

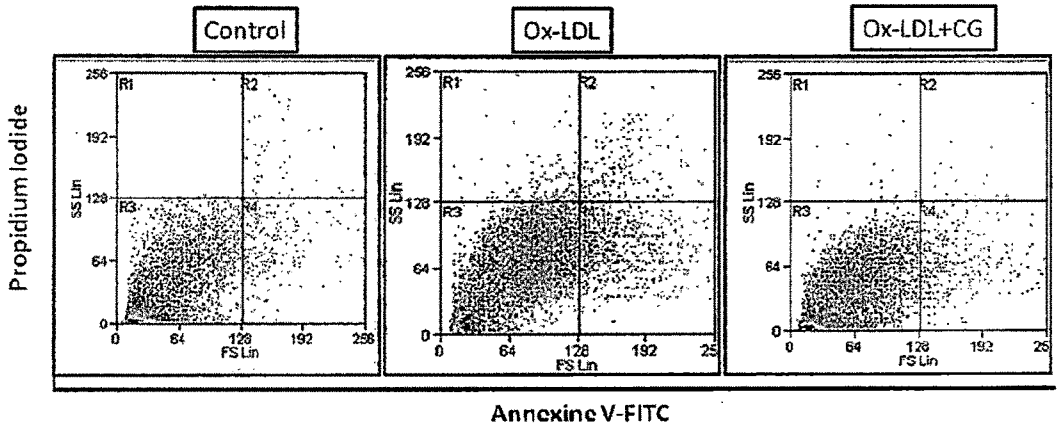

Control; HMDMs cells, Ox-LDL; HMDMs exposed to Ox-LDL and Ox-LDL+CG; HMDMs exposed to Ox-LDL in presence of 200µg/ml CG extract.

Where, R1: necrotic cells ($FITC^{-}PI^{+}$), R2: late apoptotic ($FITC^{+}PI^{+}$), R3: live cells ($FITC^{-}PI^{-}$) and R4: early apoptotic ($FITC^{+}PI^{-}$).

DISCUSSION

Oxidation of lipoproteins occurs by a variety of oxidants or multiple enzymatic or non-enzymatic pathways. Macrophages, endothelial cells and smooth muscle cells release ROS that primarily target PUFA. LDL oxidation kinetics occurs in three phases: an initial lag phase, a mid-propagation phase and a late decomposition phase (Esterbauer *et al.* 1989). Oxidation of LDL is a free radical driven lipid peroxidation process initiated by the removal of hydrogen atom from a methylene (CH_2) group of PUFA moiety of LDL. The resultant carbon atom is unstable and undergoes molecular rearrangement to form more stable configuration, a conjugated diene (CD). In subsequent steps, CD reacts with molecular oxygen to form peroxyl radical that further abstracts hydrogen atom form adjacent PUFA and cholesterol to form LHP and oxysterols respectively. This LHP undergoes further fragmentation to short chain aldehydes i.e. MDA and 4-hydroxynonenal. Subsequently, these aldehydes bring about modification of the ApoB in LDL by formation of covalent adduct with its lysine residue. This event introduces a negative charge to the LDL molecule that makes it recognizable by the scavenger receptor of macrophages, resulting in increased LDL uptake by macrophages and their transformation into foam cells (Young and McEneny, 2001). This is a hallmark prelude to onset of atherosclerosis.

The propagation phase of LDL oxidation begins with the depletion of endogenous antioxidants (α-tocopherol, ubiquinol-10, β-carotene and retinol). In the present study, CG extract recorded prolonged lag phase in Cu^{2+} mediated LDL oxidation kinetics, reduced rate of oxidation and lowered CD_{max}. These results are attributable to the established metal chelating and free radical scavenging property of CG extract (Jadeja *et al.*, 2009b). However, possible preservation of endogenous LDL antioxidants (Vitamin E and A) in presence of CG extract, cannot be ruled out and

requires further scrutiny. Moreover, significant reduction in the formation of various intermediaries of LDL oxidation (MDA, CD and PC) suggests a possible chain breaking antioxidant role for CG extract. A rich content of polyphenols and flavonoids shown in CG extract by our previous studies (Chapter 1) could be considered to prevent Ox-LDL induced ApoB fragmentation in presence of CG extract as has also been suggested by Berrougui *et al.* (2006). There is substantial evidence for the presence of oxLDL within arterial walls with atherosclerotic lesion, not characteristic of normal arterial walls (Chisolm and Steinberg, 2000). LDL that is extracted from human and animal atherosclerotic lesions is characteristically similar to the ox-LDL formed by cell-mediated oxidation of LDL in culture (Yla-Herttuala *et al.*, 1989). Macrophages, smooth muscle cells, and endothelial cells are reportedly key players in this process, driven by either ROS or myeloperoxidase (Asmis and Begley, 2003). In the present study, nLDL underwent oxidation when incubated with HMDMs while, presence of CG extract minimized the same as evidenced from the reduced indices of MDA and CD. Prevention of cell mediated LDL oxidation by CG extract is attributable to its high content of flavonoids and polyphenols as reported earlier (Frankel *et al.*, 1993; Aviram and Fuhrman, 1998).

Cellular uptake of Ox-LDL and subsequent production of peroxyl radical precede apoptosis of macrophages during induction of atherosclerosis (Asmis and Begley, 2003). An increase in intracellular load of peroxyl radicals is indicted by the higher number of DCF-DA positive cells on exposure of HMDMs to Ox-LDL. Interestingly, Ox-LDL induced generation of peroxyl radicals in HMDMs seems significantly attenuated in presence of CG extract. These observations are correlatable with the observed reduction in uptake of Ox-LDL in presence of CG extract, eventually contributing to minimal production of peroxyl radicals.

Disruption of mitochondrial function by Ox-LDL is attributed to peroxyl radicals (Asmis and Begley, 2003) and, these radicals cause peroxidation of mitochondrial membrane lipids resulting in collapse of membrane potential and subsequent uncoupling of respiratory chain (Asmis and Begley, 2003). Presently observed collapse of mitochondrial membrane potential in Ox-LDL exposed HMDMs is in accordance with the previous reports (Asmis and Begley, 2003). However, co-presence of CG extract minimized the changes in mitochondrial membrane potential, indicating the ability of CG extract in maintaining mitochondrial integrity. This property of CG is in accordance with our previous report on the ability of CG extract to safeguard mitochondrial function in a mouse model of steatohepatitis, primarily due to its ability to scavange peroxyl radicals (Chapter 2).

It is likely that during early atherosclerotic lesions, neighbouring macrophages help clear the apoptotic macrophages. However, during the later stages of atherosclerotic progression, inefficiency of macrophages apoptosis and phagocytic clearance leads to secondary necrosis of the macrophages, leading to the formation of a necrotic core that promotes further inflammation and acute thrombotic lesion culminating in plaque instability (Kockx, 1998; Tabas, 2005). This sequence of events in human and experimental animals clearly suggests oxidation of LDL and subsequent Ox-LDL induced apoptosis of macrophages to be the key events during atherogenesis (Kockx and Herman, 2000; Stoneman and Bennett, 2004). However, evaluation of preventive/reversible effect of any herbal/synthetic therapeutic agent *in vivo* poses a difficult paradigm. The protocol employed herein replicates the same set of events *in vitro* in which, the extent of apoptosis helps in determining Ox-LDL induced cytotoxicity. In the present study, HMDMs show reduced cell viability after 24 hr, suggesting the onset of Ox-LDL induced cytotoxicity. Flow cytometric analysis of

cell cycle indicates a paradigm shift towards sub-G0 phase thus confirming induction of apoptosis. These observations stand further substantiated by the recorded significantly more number of annexin V-FITC positive cells and, nuclear condensation as confirmed by DAPI staining. Moreover, the protective role of CG extract as revealed by the healthy and functional nuclear morphology also stand confirmed by the observed lesser percentage of cells in sub-G0 phase as marked by the lesser degree of annexin V-FITC positivity

Finally, it is inerrable from the current study that CG extract has the potential of preventing LDL oxidation and Ox-LDL induced apoptosis of HMDMs. These results are attributable to the antioxidant potential and free radical scavenging property of CG extract. This being the first detailed scientific report that infers anti-atherosclerotic potential of CG extract, provides further validity to its multi-therapeutic potentials besides its already established folklore medicinal value.

Summary

This study reports the protective role of *Clerodendron glandulosum* (CG) extract against *in vitro* LDL oxidation and Ox-LDL induced macrophage apoptosis using various experimental models. Effect of CG extract on Cu^{2+} mediated LDL oxidation kinetics and formation of various intermediary products and its ability to prevent human monocyte derived macrophage mediated LDL oxidation have been investigated. Ox-LDL induced macrophage apoptosis was evaluated by nuclear condensation, cell cycle analysis, and annexinV-FITC/PI staining in presence or absence of CG extract. Results recorded in the present study clearly suggest the protective role of CG extract against LDL oxidation and Ox-LDL induced macrophage oxidative stress, mitochondrial dysfunction, and apoptosis. This is the first report on the protective role of CG extract on two key events of atherosclerosis portending its possible therapeutic use as an anti-atherogenic herbal medicine.